AIAA JOURNAL
Vol. 32, No. 7, July 1994

# Response of Hot-Element Wall Shear Stress Gages in Unsteady Turbulent Flows

W. J. Cook*
*Iowa State University, Ames, Iowa 50011*

**Experimentally determined response characteristics of two types of hot-element wall shear stress gages are described for unsteady turbulent flows. One is the substrate-type thin-film gage and the other is a gage with a small cavity below a surface-level thin-film quartz-fiber element. Two substrate-type gages were tested: a quartz-substrate gage, and a glue-on gage with a thin flexible substrate. Steady-flow gage calibrations were used in reducing unsteady flow data. The cavity gage showed excellent response to a steplike flow, whereas the two substrate gages exhibited response times on the order of tens of seconds for the same flow. Steady-flow shear stress turbulence levels indicated by the cavity and substrate gages were 28 and 12%, respectively. In oscillating flows the substrate gages indicated lagging shear stress variations with significantly reduced amplitudes for oscillation frequencies ranging from 3 to 12 Hz, whereas the cavity gage exhibited a much more rapid response. Results indicate that the substrate gages register correct variations only for very low frequencies of oscillation.**

## Nomenclature

$A$ = calibration constant, Eq. (2)
$E$ = anemometer output voltage
$E_0$ = zero-flow anemometer output voltage
$f$ = frequency, Hz
$G$ = $X^2/\Delta f$
$H$ = boundary-layer shape factor, $\delta^*/\theta$
$L$ = dimension of hot element in flow direction
$L^+$ = $L/\eta^*$
$N$ = calibration constant, Eq. (2)
$R_0$ = hot-element resistance at room temperature
$R_{\text{Hot}}$ = hot-element resistance at operating temperature
$Re_\theta$ = momentum thickness Reynolds number
$t$ = time
$U$ = freestream velocity
$u$ = $x$ component of boundary-layer velocity
$u_\tau$ = friction velocity, $(\tau_s/\rho)^{1/2}$
$u^+$ = $u/u_\tau$
$W$ = dimension of hot element perpendicular to flow direction
$W^+$ = $W/\eta^*$
$X$ = amplitude in Fourier series
$x$ = length measured parallel to wall in the flow direction
$y$ = length measured perpendicular to wall
$y^+$ = $y/\eta^*$
$\delta_s$ = steady-flow boundary-layer thickness at 99% of $U_s$
$\delta^*$ = steady-flow boundary-layer displacement thickness
$\eta^*$ = $\upsilon/u_\tau$
$\theta$ = steady-flow boundary-layer momentum thickness
$\nu$ = $\mu/\rho$
$\sigma$ = standard deviation of steady-flow wall shear stress fluctuations
$\tau$ = wall shear stress
$\phi_c$ = additive correction to $\phi_\tau$
$\phi_u$ = velocity phase angle, Eq. (4)
$\phi_\tau$ = wall shear stress phase angle, Eq. (5)
$\omega$ = angular frequency, $2\pi f$

*Subscripts*

$m$ = mean of ensemble-averaged quantity
$s$ = steady flow
1 = amplitude of ensemble-averaged quantity
1$c$ = corrected amplitude

Presented as Paper 91-0167 at the AIAA 29th Aerospace Sciences Meeting, Reno, NV, Jan. 7–10, 1991; received April 6, 1993; revision received Nov. 8, 1993; accepted for publication Nov. 16, 1993. 

*Professor, Department of Mechanical Engineering. Member AIAA.

## I. Introduction

A MEANS for measuring wall shear stress in both steady and unsteady flows is of significant interest in aerodynamics. Several instruments and techniques are available for flows that are steady.[1,2] However, few of these have response times adequate for measuring time-varying wall shear stresses. One exception appears to be the hot-element gage. This instrument seems in many respects to be ideal because it is small, rugged, inexpensive, and relatively simple to operate. Although the gage shows promise for measuring unsteady shear stress variations, questions remain as to the adequacy of its time response and the interpretation of its signals. A few studies, both analytical and experimental, dealing with response characteristics of these gages have been reported in the literature. Analytical efforts have been made to predict gage response, but these are in the early stages of development; e.g., see Cole and Beck.[3] Because of the complexity of the time-dependent heat transfer processes associated with gage operation, experimental studies are useful to provide practical results and to supply modelers with experimental response information against which predictions can be checked. Cook et al.[4] conducted an experimental study of the response of substrate-type hot-element gages for laminar oscillating flows and demonstrated through an examination of the phase relationship of the response that these gages exhibit a significant time lag in such flows. Alfredsson et al.[5] recently carried out a study of the fluctuation in wall shear stress in steady turbulent flows using substrate-type hot-element gages and found significant dynamic response difficulties with the gages when they are used to measure shear stress fluctuations in air.[5] In the present study, an experimental investigation was undertaken to further examine the response characteristics of hot-element gages in unsteady airflows. This study has focused on the response characteristics of two types of hot-element wall shear stress gages operated in time-dependent turbulent flows in the incompressible flow regime.

## II. Description of Hot-Element Gages Studied

The hot-element gage used as a wall shear stress measuring instrument is operated by a constant-temperature anemometer unit. The active element is maintained at a constant elevated temperature by the unit. The anemometer decade resistance setting establishes the element operating resistance and in turn dictates its operating temperature. Calibration of the system is required if wall shear stress is to be measured. The two types of hot-element wall

shear stress gages examined during this investigation are the substrate-type hot-element gage and a somewhat similar gage that will be referred to as the "cavity" hot-element gage.

The substrate hot-element gage consists of a thin metallic film deposited on a substrate, the surface of which is mounted flush with the surface on which the shear stress is to be measured. References 6–11 provide background and information related to this instrument. Substrate gages are commercially available in two substrate configurations: the quartz-substrate gage for which the film is deposited on a thick quartz substrate and the glue-on gage prepared by depositing a metallic film on a thin flexible polymer backing strip that is glued to a surface. These configurations are illustrated in Fig. 1a.

Shown is the Thermal Systems Inc. (TSI) model 1237 flush-mounted probe and the glue-on DANTEC 55R47 gage. The former configuration is practical where size restrictions are not severe. The latter configuration is of considerable practical utility since the substrate is thin and flexible, and thus the gage can be mounted on surfaces of aerodynamic testing models and other surfaces such as compressor blades. Both types have been used without calibration as instruments to detect flow separation, boundary-layer transition, and other similar events. See, for example, the study by Stack et al.[12] in which flexible-substrate hot-element gages were used to detect laminar boundary layer separation on an airfoil.

From previous studies it is clear that heat conduction to the substrate adversely affects the time response of substrate-type hot-element gages. Some work has been done in gage design to decrease substrate heat transfer. McCroskey and Durbin[13] and Houdeville et al.[14] used a surface-level hot element mounted above a small cavity to achieve reduced substrate heat transfer. The cavity gage as described in Ref. 14 is illustrated in Fig. 1b. Results of each of the noted studies indicate that reduced substrate heat transfer was achieved. Houdeville et al. carried out limited testing of the cavity gage for both laminar and turbulent oscillating flows. Their results suggest that the response characteristics of the cavity gage are considerably better than the substrate-type gages. Drawbacks of the cavity gage include increased gage construction complexity and fragility relative to substrate-type hot-element gages. The cavity gage is not commercially available.

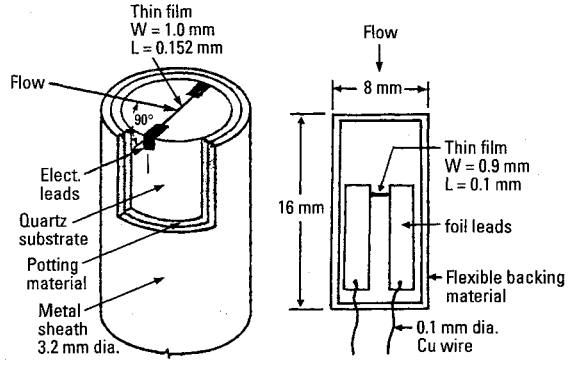


a) Substrate gages

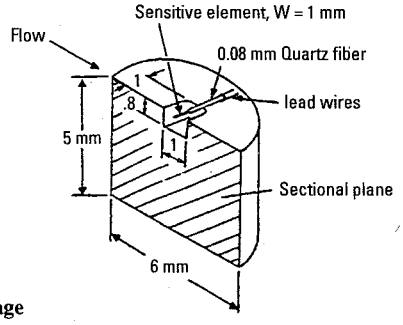


b) Cavity gage

**Fig. 1 Description of hot-element gages.**

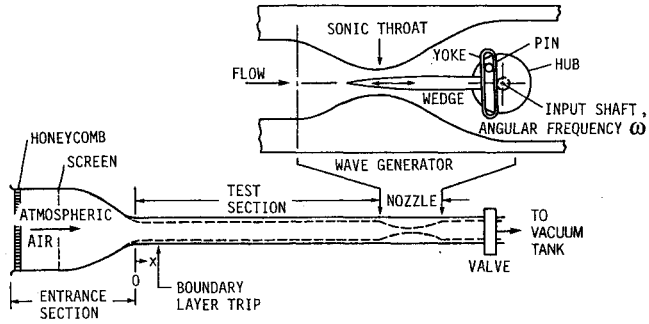


**Fig. 2 Description of test facility.**

## III. Test Facility

Well-controlled repeatable unsteady test flows are necessary to experimentally investigate the response characteristics of hot-element gages. Such flows were produced in the present study by the facility illustrated in Fig. 2. The facility consists of an entrance section and a test section of square cross section (7.5 × 7.5 cm) that is terminated at a length of 2 m by a nozzle that has a two-dimensional contour. Atmospheric air is the test medium, and the facility is vacuum driven. The nozzle discharge region pressure is sufficiently low during testing to maintain sonic flow at the nozzle throat. A significant advantage of the sonic throat is that it isolates the test section from downstream flow disturbances. This, coupled with a properly designed entrance section, produces test section flows that have a minimum of extraneous flow disturbances. Three types of flows were generated for this investigation: steady flows, steplike flows, and periodic flows. Steady flows were produced by locking the wave-generator wedge at fixed positions. The steplike flows were created by rapidly opening the valve between the facility and the vacuum tank with the wedge in a fixed position. Periodic flows were generated by operating the wave generator during flow. This produced test section freestream flows that are characterized by a nonzero mean velocity with a superposed periodic component produced by the wedge motion. A properly shaped wedge produces an essentially true sinusoidal test section velocity variation at any fixed frequency ranging from values close to zero to about 50 Hz.

Experiments to evaluate the response of the hot-element gages were conducted by measuring the shear stress variation on the wall of the test facility 0.91 m from the boundary-layer trips positioned at $x = 0.13$ m (Fig. 2). The trips were used to insure that the wall boundary layer was turbulent. Periodic-flow experiments were conducted at frequencies ranging from 3 to 12 Hz. At the test location the mean freestream velocity $U_m$ and the amplitude $U_1$ were, respectively, 21.9 and 3.11 m/s. The capacity of the vacuum pump used to drive the system was sufficient to produce continuous flows at the conditions noted.

To establish a reference flow and to evaluate the corresponding wall shear stress, a boundary-layer velocity survey was performed using a hot-wire anemometer with the wedge locked at midstroke, which produced steady test-section flow with $U_m = 21.9$ m/s. The hot-wire probe used was a DANTEC 55P14 right-angle single-wire probe that was traversed through the test-section wall. The probe-traversing mechanism incorporated a micrometer with a least count of 0.025 mm (0.001 in.). The anemometer system consisted of a DANTEC 55M10 main unit, a DANTEC 55D10 linearizer, and a General Radio type 1952 filter. The system output voltage was read by a National Instruments Corporation data acquisition board driven by an IBM System 2 model 50Z computer. The anemometer system was calibrated using a TSI model 1125 airflow calibrator to a voltage range that matched the most sensitive voltage range of the data acquisition board. A more detailed description of the techniques used is given in Ref. 15.

The steady-flow boundary layer velocity thickness $\delta_s$ was determined to be 1.8 cm, and the value of $Re_\theta$ was $2.7 \times 10^3$. The results of the boundary-layer survey in terms of law-of-the-wall coordinates $u^+$ vs $y^+$ showed excellent agreement with the linear-region

**Table 1 Hot-element gage calibration values; use of Eq. (2) and the constants listed yields $\tau_s$ in N/m²**

| Gage | $R_0$, Ω | OHR[a] | $E_0$, V | $A$ | $N$ |
|---|---|---|---|---|---|
| Cavity | 7.06 | 1.50 | 2.420 | 3.899 | 2.083 |
| Quartz-substrate | 5.55 | 1.15 | 8.525 | 6.053 | 2.927 |
| (TSI 1237) | 5.55 | 1.30 | 12.403 | 12.831 | 3.117 |
| Glue-on (Dantec 55R47) | 15.60 | 1.20 | 2.321 | 1.481 | 2.903 |

[a]OHR = overheat ratio = $R_{hot}/R_0$

equation $u^+ = (1/0.41)\ \ell n(y^+) + 5.0$. The friction velocity $u_\tau$ was determined using the wall shear stress $\tau_s$ obtained from the skin friction expression of Ludwieg and Tillman[16]:

$$C_f = \tau_s/(\rho U_m^2/2) = 0.246 \times 10^{-0.678H}/Re_\theta^{0.268} \quad (1)$$

The quantitites $\delta^*$ and $\theta$ were determined from integration of measured velocity profile data.

## IV. Gage Calibration

Although the present study deals with measurement of unsteady wall shear stress variations, calibration of the hot-element gages for steady flows is introduced here with the view that a steady flow calibration for an instrument with very fast response (such as an anemometer equipped with a hot-wire probe) will also serve for unsteady flows. The adequacy of response can then be assessed by examining the degree to which wall shear stress variations obtained using the steady-flow calibration agree with the actual unsteady wall shear stress variations. The wall shear stress for steady flows $\tau_s$ is related to the anemometer output voltage $E$ by the expression

$$E^2 = E_0^2 + A\,\tau_s^{1/N} \quad (2)$$

For substrate gages, $N$ is typically about 3. The basic theory of gage operation given by Eq. (2) has been successfully used to obtain sensor calibrations for measurement of $\tau_s$ in a wide variety of steady flows; e.g., see the studies described in Refs. 5–11, 13, and 17.

In the present study, the gages were prepared for exposure to the test flow by mounting their hot-element surfaces flush with the surfaces of wall plugs, the test surfaces of which were closely matched with the inner wall of the test section. The estimated mismatch of the plug test surfaces with the wall was ±0.025 mm (±0.001 in.). The quartz-substrate gage and the cavity gages were mounted in aluminum wall plugs through closely fitting holes. The glue-on gage was glued directly to the test surface of a Lexan plug using quick-setting epoxy glue. The gage surface was not recessed below the plug surface, and as a result, the gage protruded into the flow by the thickness of the flexible substrate, about 0.025 mm (0.001 in.).

To calibrate the hot-element gages, the facility was operated at three steady-flow conditions: the first with the wedge locked in its most upstream position (producing the minimum flow velocity, 18.8 m/s), the second with the wedge locked at midstroke (21.9 m/s), and the third with the wedge locked in the fully downstream position, producing the maximum flow velocity (25.0 m/s). Boundary-layer velocity surveys were made for these three flows, and the results were processed using Eq. (1) to obtain the wall shear stress for each flow. The data acquisition system for the hot-element gages consisted of the main anemometer unit connected to the data acquisition board through a dc voltage source that was used to apply a constant negative dc biasing voltage to the positive signal from the main anemometer unit (typically several volts) to reduce the signal measured by the data acquisition board to the range of 0–1.25 V. This provided the maximum signal resolution available from the 12-bit analog-to-digital converter: 0.305 mV. The biasing voltage was then added to the board voltage readings by the computer during data processing. The hot-element gages were individually connected to the anemometer and exposed to the flows to obtain calibration voltage measurements.

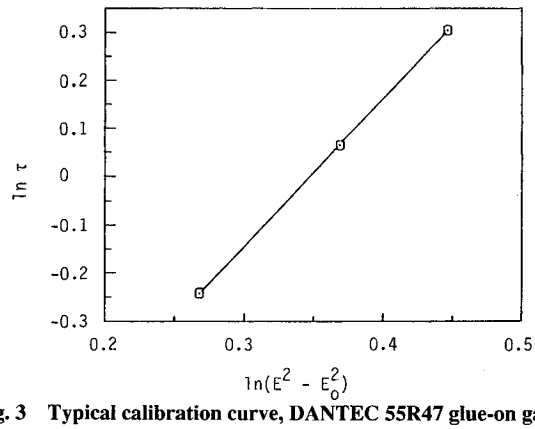


**Fig. 3 Typical calibration curve, DANTEC 55R47 glue-on gage.**

The overheat ratios at which the gages were calibrated and operated are listed in Table 1. The voltage reading for $E_0$ for an energized gage was taken by the data acquisition system after its value became stable. The flow was then initiated, and the voltage $E$ in Eq. (2) was measured for each of the three steady flows after stable mean values for gage voltage were obtained. Because a high turbulence level existed for the wall shear stress, voltage values were determined by taking the mean of a large number of voltage readings. A least-squares fit of $\ell n(\tau_s)$ to $\ell n(E^2 - E_0^2)$ for the three points for each gage provided the calibration constants $A$ and $N$. Figure 3 shows a typical calibration curve. Values obtained for the constants $A$ and $N$ are listed in Table 1.

## V. Gage Response for a Steplike Flow

As noted, a steplike flow was generated in the test facility by rapidly opening the valve between the evacuated vacuum tank and the test facility. The wedge of the wave generator was locked at midstroke for this flow. This produced a steady value of $U$ at the test location equal to 21.9 m/s. The time-dependent flow velocity associated with flow initiation was measured using a hot-wire probe positioned on the test section centerline at the test location. Figure 4a shows the velocity measured by the hot-wire probe vs time. Time equals zero corresponds to flow initiation. The figure shows that transients due to wave reflections in the test section produced by the sudden flow initiation completely disappeared by 0.3 s after the flow was started. Thus, when times on the order of seconds are considered, the flow is essentially a step in freestream velocity.

The response of each hot-element gage to the steplike flow was measured. In each case the steady flow gage calibration constants listed in Table 1 were used in computing $\tau$ values from transient voltage data recorded by the data acquisition system. Each gage was subjected to this flow only after it was energized and had reached its stable zero-flow voltage value. For the substrate gages the time required to attain stable zero-flow voltage readings was about 2 min. Figure 4b shows the gage response for the cavity gage in terms of wall shear stress vs time. The points in the figure were calculated from voltage records taken at a sampling rate of 500 points/s. The results show an early-time transient followed by the immediate onset of a shear stress with a high turbulence level. The shear stress rapidly reaches the time steady value $\tau_s$ indicated in Fig. 4b by the solid line. Values for $\tau_s$ and the ratio $\sigma/\tau_s$ and other related quantities are shown in Table 2; $\sigma$ is the standard deviation of the wall shear stress fluctuations about the mean $\tau_s$.

Times beyond 80 s were required for the substrate gages to register time-steady values for the mean wall shear stress. Figures 4c and 4d present the responses of the TSI 1237 quartz-substrate and the DANTEC 55R47 glue-on gages respectively. The solid curves were obtained by averaging values over short time intervals. As noted in Table 1, the quartz-substrate gage was operated at two overheat ratios: 1.15 and 1.3. No influence of overheat ratio was

detected for either the steplike flow or for the oscillating flows that are described in subsequent sections. Values for $\tau_s$ and $\sigma/\tau_s$ are listed in Table 2 for the quartz-substrate and glue-on gages. It is evident from Figs. 4c and 4d that the response times to the step flow for the substrate gages, as given by the time required for either substrate-type gage to indicate a time-steady mean shear stress, are very long compared with that for the cavity gage. In addition, the time required for the quartz substrate gage to reach 90% of $\tau_s$ is 32 s, whereas the corresponding time for the glue-on gage is 19 s. Thus, the glue-on gage has a somewhat faster mean response to the steplike flow.

The values of $\tau_s$ in Table 2 for the three gages are nearly the same, but the standard deviations of shear stresses differ considerably. Extensive measurements made by Alfredsson et al.[5] in turbulent water, oil, and airflows indicate that, for a turbulent boundary layer, $\sigma/\tau_s$ is 0.40. These authors also demonstrate that the dynamic response of a hot-element gage depends on at least two factors: the nature of the heat transfer from the hot element and the length of the hot element in the transverse flow direction. Heat transfer to the substrate should be small compared with that to the fluid, and for adequate spatial resolution, $W^+ = W/\eta^*$, the dimensionless transverse length of the hot element, should be less than about 10–20. Table 2 lists the values of $W^+$ for the three gages. (Values for $L^+$ are typically small; Table 2 shows that $L^+$ is less than 10 for the present gages.) For the cavity gage, heat transfer to the fluid is large compared with that to the substrate, but the value of 61 for $W^+$ for this gage indicates that it lacks spatial resolution in the test flows. Hence the value obtained for $\sigma/\tau_s$ was 0.28 instead of the expected value 0.40. The lower values of $\sigma/\tau_s$ indicated by the two substrate-type gages is explained by impaired dynamic response caused by the large values of $W^+$ for these gages and the fact that the heat transfer from the gage is dominated by conduction into the substrate. Substrate-gage measurements by other investigators[5] yielded values for $\sigma/\tau_s$ that range between 0.06 and 0.12 for airflows.

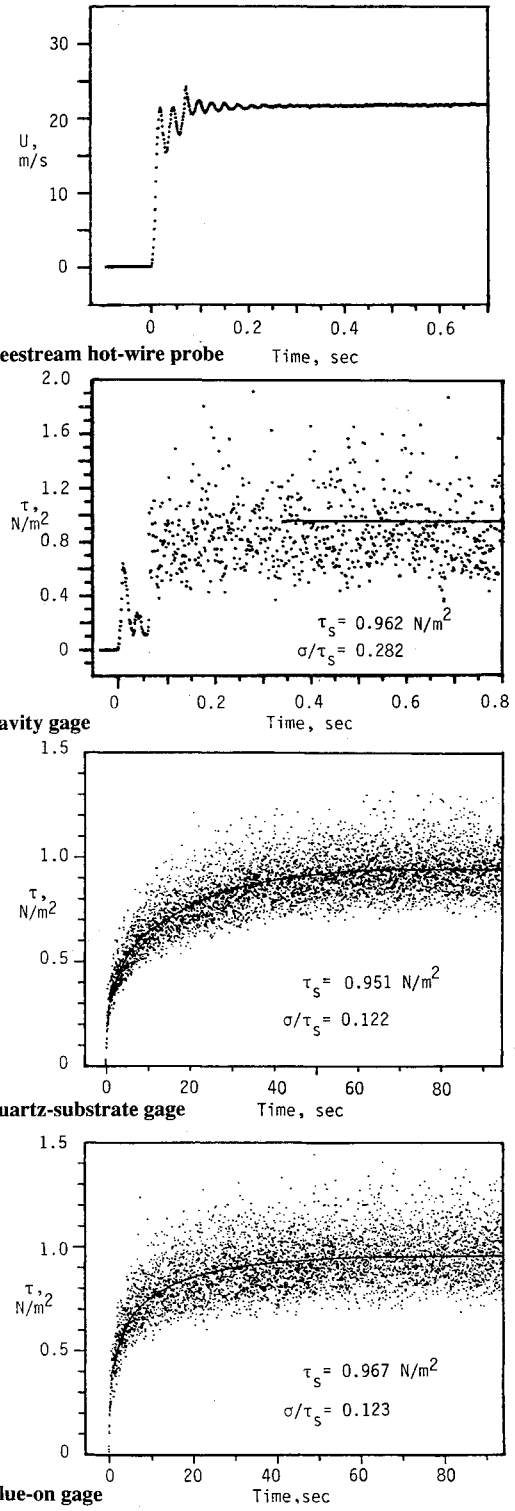


**Fig. 4 Instrument responses to a steplike flow.**

**Table 2 Quantities related to steady wall shear stress measurements; $Re_\theta = 2.7 \times 10^3$**

| Gage | $\tau_s$, Pa | $\sigma/\tau_s$ | $L^+$ | $W^+$ | Skewness | Flatness |
|---|---|---|---|---|---|---|
| Cavity | 0.962 | 0.282 | 5.0 | 61 | 0.95 | 4.43 |
| Quartz-substrate | 0.951 | 0.122 | 9.5 | 61 | —— | —— |
| Glue-on | 0.967 | 0.123 | 6.2 | 55 | 0.61 | 3.45 |

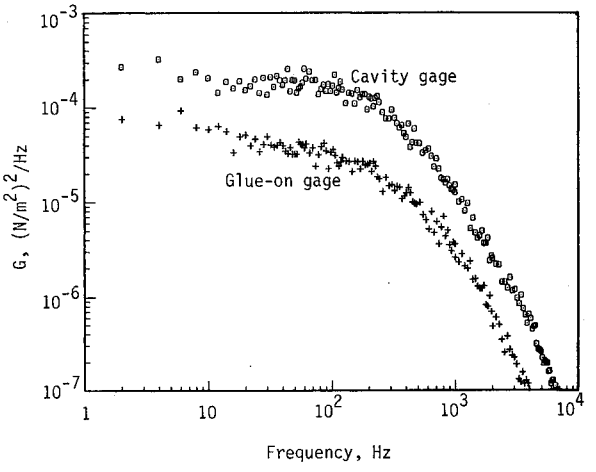


**Fig. 5 Spectra of wall shear stress measurements for two hot-element gages.**

Values in Table 2 for skewness and flatness from the cavity gage measurements, 0.95 and 4.43, respectively, are close to the values 1.0 and 4.8 obtained by Alfredsson et al. The skewness and flatness values in Table 2 for the glue-on gage are smaller than those for the cavity gage. These diminished values are consistent with the diminished values of $\sigma/\tau_s$ for the glue-on gage.

The possibility exists that the cavity below the hot element of the cavity gage could interact dynamically with the flow and thus yield a false reading. To investigate this, data were taken during steady-flow operation to obtain shear stress turbulence spectra for both the cavity gage and the glue-on gage. The results for each gage are shown in Fig. 5 in terms of $G$ vs frequency, where $G$ is the square of shear stress fluctuation per unit frequency at a given frequency. The spectra for both gages are somewhat similar to those obtained for velocity fluctuations in turbulent flows. The lower values of $G(f)$ for the glue-on gage are consistent with its impaired dynamic response. Within the scatter, the results for the cavity gage show no sharp increases or decreases in amplitudes for

the frequency range shown. Thus there is no spectral evidence of an interaction between the cavity and the flow.

## VI. Oscillating Flow Description

In addition to studying the hot-element gage response to the steplike flow, the response of the gages was examined for oscillating (periodic) flows with frequencies ranging from 3 to 12 Hz. This section describes the nature of the oscillating flows generated and the means by which the actual wall shear stress variations were determined. As will become evident, to obtain the actual wall shear stress variation, this study has relied to a significant degree on information obtained from experimental velocity profile data that describe the periodic boundary-layer flows generated.

### Boundary-Layer Velocity Variation

As noted, the periodic freestream flow produced by the test facility consists of a mean flow with a superposed sinusoidal variation. The freestream velocity variation at the test location can be written as

$$U(t) = U_m + U_1\cos(\omega t) \tag{3}$$

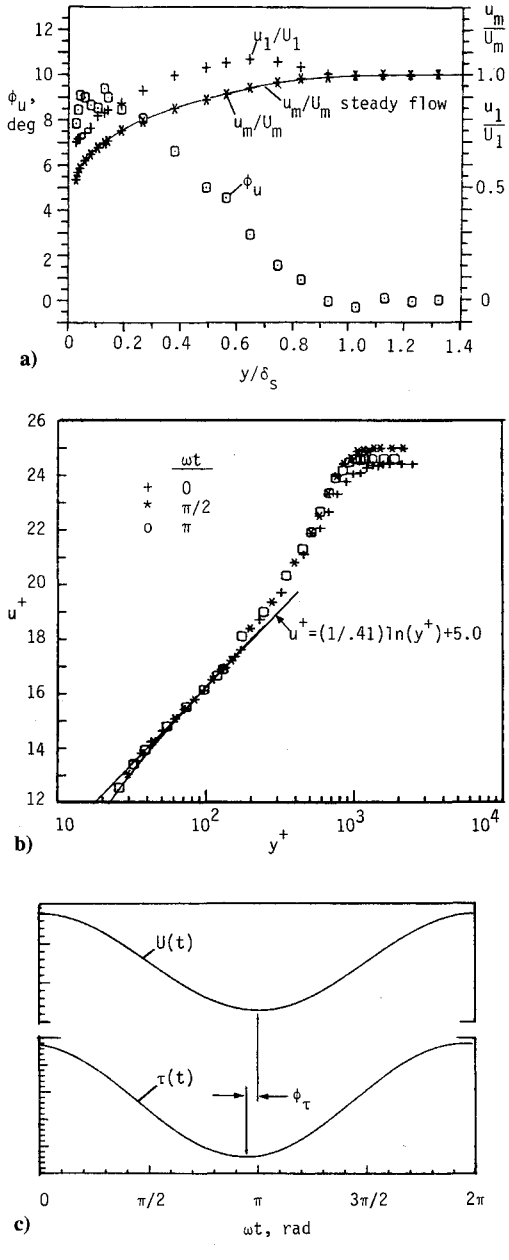


**Fig. 6 Evaluation of $\tau(t)$ from the processing of instantaneous velocity profiles, $f = 6$ Hz.**

The corresponding velocity variation in the boundary layer has the form

$$u(y, t) = u_m(y) + u_1(y)\cos[\omega t + \phi_u(y)] \tag{4}$$

In Eq. (4), $\phi_u(y)$ denotes the phase angle by which $u(y, t)$ leads $U(t)$. For turbulent flows in which large turbulent fluctuations are present, the velocity exhibits a significantly different variation each cycle of oscillation. Therefore, the subscripted quantities of Eqs. (3) and (4) are interpreted as ensemble (phased) averaged values. Such values are obtained by averaging results over a large number of cycles. The technique used to obtain a description of oscillating flows involved making measurements for a large number of cycles of oscillation through the use of the external trigger capabilities of the data acquisition system. The wave generator mechanism, Fig. 2, is equipped with a BEI Electronics Corp. encoder that is driven at wave generator drive-shaft speed. It produces a once-per-revolution signal to provide an external trigger signal to the data acquisition board and another signal consisting of 1440 pulses per revolution. The latter signal was used in conjunction with an electronic pulse counter to determine the angular frequency of the wave generator drive shaft. This and an adjustable-speed drive motor permitted the wave generator frequency to be accurately set. Software for the data acquisition board permitted the board to be configured to take bursts of anemometer voltage readings equally spaced in time for each once-per-revolution external trigger received. The delay between readings was set to obtain an integer number of readings per period of oscillation. After acquiring data for a large number of cycles, the data at each cycle point were processed to obtain ensemble-averaged results for the cycle. Sine wave curves were then fitted to the results at various $y$ locations across the boundary layer. The results obtained showed that a very precise sinusoidal velocity variation is produced by the facility. Equations for the fitted curves permitted convenient and accurate evaluation of amplitudes and phase angles.

Figure 6a presents in dimensionless form the results for a complete oscillating flow survey obtained at a frequency of 6 Hz. Results are shown in terms of the ratios $u_m/U_m$, $u_1/U_1$, and the phase angle $\phi_u$ vs $y/\delta_s$, where $\delta_s$ was measured with the wedge locked at midstroke. Also shown is $u_m/U_m$ from a corresponding steady-flow velocity survey. The agreement between this profile and the $u_m/U_m$ results for the oscillating flow is good throughout the $y/\delta_s$ range, thereby indicating that the oscillation did not influence the mean velocity profile. However, unsteadiness in the flow is evident from the variation in the velocity phase angle $\phi_u$ across the boundary layer and the fact that the amplitude ratio $u_1/U_1$ exceeds unity in the boundary layer. These results are similar to those obtained by other investigators, e.g., Patel[18] and Cousteix et al.[19]

### Wall Shear Stress Variation

The ensemble-averaged wall shear stress also behaves in an unsteady manner in a periodic flow. For small velocity amplitudes, its variation can be written as

$$\tau(t) = \tau_m + \tau_1\cos(\omega t + \phi_\tau) \tag{5}$$

where a positive value for $\phi_\tau$ indicates that $\tau(t)$ leads the freestream velocity $U(t)$, Eq. (3). To assess the response characteristics of the hot-element gages, it is of course necessary to know the actual wall shear stress variation as described by Eq. (5). Although exact solutions to the unsteady boundary-layer equations would deliver the wall shear stress variation, such solutions are not available. Two other methods were used in the present study to obtain the unsteady wall shear stress variation.

### Shear Stress from Instantaneous Velocity Profiles

It is well known that for steady incompressible turbulent boundary-layer flows wall shear stress can be determined from velocity profile information alone if the velocity profile exhibits a linear region on a plot of $u^+$ vs $\ell n(y^+)$. This applies to incompressible steady turbulent boundary-layer flows over a wide range of Reynolds number[20] and with pressure gradients ranging from strongly favorable to strongly adverse.[21] Houdeville et al.[14] have applied

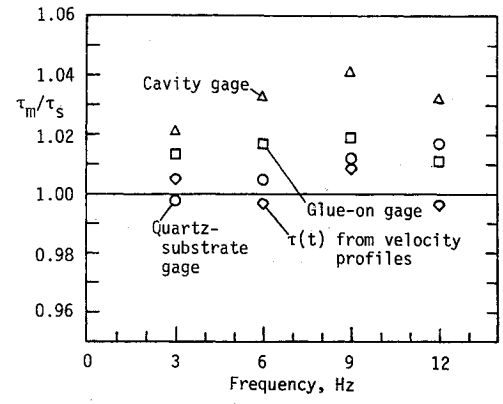


a) Comparison of values for $\tau_m/\tau_s$

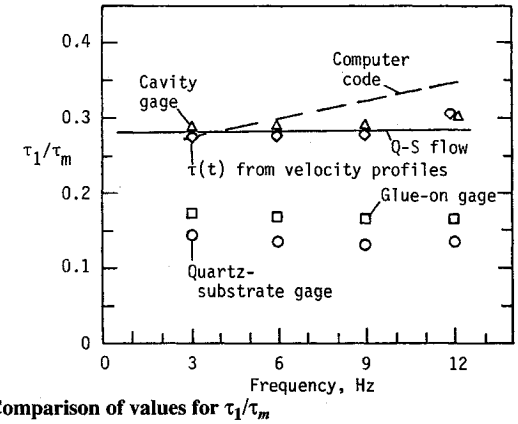


b) Comparison of values for $\tau_1/\tau_m$

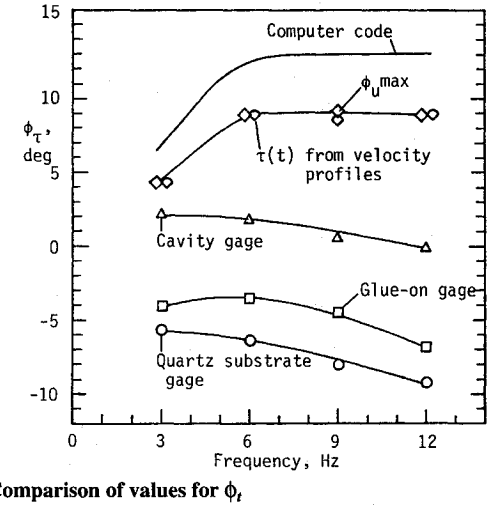


c) Comparison of values for $\phi_t$

**Fig. 7 Comparison of wall shear stress quantities for oscillating flows.**

this technique to instantaneous velocity profiles for oscillating flows to determine the wall shear stress variation with time in an oscillating turbulent boundary-layer flow and have found that it gives satisfactory wall shear stress variations for low-frequency oscillating flows.[14] Application of the method to the present study involved use of experimental unsteady velocity profile results like those in Fig. 6a. Equation (4) was used in conjunction with such results to generate 20 instantaneous velocity profiles at values of $\omega t$ in the range zero to $2\pi$. Each was treated as a steady profile, and integrations were performed to obtain $H$ and $Re_\theta$. Equation (1) was then applied to determine the 20 corresponding values for $\tau$. Figure 6b shows in terms of $u^+$ and $y^+$ instantaneous velocity profiles generated at three $\omega t$ values for the oscillating flow at 6 Hz. The profiles match the steady-flow reference curve well in a portion of the linear region. Figure 6c shows a typical variation in wall shear stress computed in this manner and the corresponding measured freestream velocity variation. As shown in the figure, $\tau(t)$ leads $U(t)$. Thus, for oscillating flows, the actual wall shear stress variation in the form of Eq. (5) can be evaluated from measurements of unsteady velocity profiles. The wall shear stress variations were determined in this manner for oscillating flows ranging in frequency from 3 to 12 Hz.

#### Shear Stress by Numerical Computation

Computations to evaluate $\tau(t)$, Eq. (5), were carried out using the numerical method developed by Murphy and Prenter[22] for solving the unsteady turbulent boundary-layer equations for the oscillating flows. The Cebeci-Smith[23] algebraic turbulence model was used in conjunction with the computer code. Results were obtained for frequencies ranging from 3 to 12 Hz.

## VII. Gage Response for Oscillating Flows

The three hot-element gages were subjected to oscillating flows at frequencies ranging from 3 to 12 Hz to evaluate their response characteristics. The gages were operated at the overheat ratios listed in Table 1, and data were taken using the same components of the data acquisition system as were used for measuring the gage response to the steplike flow. Results for $\tau(t)$ in the form of Eq. (5) were obtained by ensemble averaging processed data taken at 100 voltage readings per cycle for 240 cycles of flow oscillation. The calibration constants in Table 1 were used to evaluate $\tau$ from the voltage readings. The external trigger to the data acquisition board was supplied by the once-per-revolution trigger from the encoder in the same manner as it was used in obtaining the boundary-layer velocity surveys for oscillating flows. In addition, the identical data acquisition setup was used to obtain the reference freestream velocity variation $U(t)$ as was used to monitor the response of the hot-element gages. This avoided phase errors that might be involved if a different instrument arrangement was used.

Results for the periodic wall shear stress indicated by each gage are presented in Fig. 7. Since the velocity variation in the oscillating flows exhibits a mean velocity profile essentially the same as that of the corresponding steady flow, it might be expected that the mean wall shear stress would be the same as that for steady flow. Figure 7a shows for each of the three gages the ratio $\tau_m/\tau_s$ vs frequency of oscillation, where $\tau_s$ is the wall shear stress indicated by the particular gage for steady flow. (The values for $\tau_s$ measured by each gage are listed in Table 2.) Also shown in Fig. 7a is the ratio of $\tau_m$ determined for the oscillating flows by the instantaneous velocity profile method to $\tau_s$, where for this case $\tau_s$ was taken as the average of the $\tau_s$ values indicated by the three gages. The collective results for $\tau_m/\tau_s$ for both the prediction and measurements range from about unity to 1.04. The uncertainty in $\tau_m/\tau_s$ for both the measurements and the prediction is estimated to be about ±3%. Thus, within the estimated uncertainties, there is no evidence of a significant influence of flow oscillation on the mean wall shear stress.

Figure 7b presents as a function of frequency predictions for the ratio of the shear stress amplitude $\tau_1$ to the mean shear stress $\tau_m$. The solid line represents the amplitude ratio determined from evaluation of $\tau$ for steady flows at the flow-velocity extremes of the test facility. This is the amplitude ratio for flows with frequencies approaching zero (quasisteady flows). Also shown in the figure are the amplitude ratios for the oscillating flow determined from the wall shear stress variation obtained by processing instantaneous velocity profiles. These results agree well with the quasisteady amplitude ratio, particularly below about 9 Hz. The broken line represents the amplitude ratio predicted by the unsteady boundary-layer computer code. The amplitude ratios obtained from both the instantaneous velocity profile method and the computer code show good agreement at 3 Hz with the quasisteady amplitude ratio. The computer code predicts an increasing amplitude ratio with increasing frequency, whereas the velocity profile method shows an increase after about 9 Hz. These two prediction methods are independent with the exception that measured values for the freestream velocity ($U_m$ and $U_1$) were used in the computer code.

Figure 7b also presents the results for $\tau_1/\tau_m$ determined from the response of each of the hot-element gages. The results produced by the cavity gage exhibit good agreement with the prediction obtained by application of the instantaneous velocity profile

method. However, the results for the two substrate-type gages indicate considerably diminished amplitude response.

Figure 7c presents a comparison of values for the phase angle $\phi_\tau$ [Eq. (5)] determined by various means. The figure shows the variation in $\phi_\tau$ with frequency determined using the unsteady boundary-layer computer code. Noted in the figure are values determined from the shear stress variation obtained by processing instantaneous velocity profiles. Also shown are values determined by yet another method. Cousteix et al.[19] argue on the basis of examining the momentum equation near the wall that $\phi_\tau$ is approximately the maximum value of $\phi_u$. These values for $\phi_\tau$ are obtained by taking the maximum value of $\phi_u$ from results for $\phi_u$ vs $y/\delta_s$ like those in Fig. 6a. The latter two predictions are in good agreement, and although the computer code results clearly show the same trend, the code predicts somewhat larger values. Nonetheless, all three predictions indicate that $\tau(t)$ leads the freestream velocity $U(t)$.

The $\phi_\tau$ values in Fig. 7c indicated by the three hot-element gages are generally smaller than the predicted results at the same frequency. The cavity gage response exhibits positive (leading) values for the frequency range examined, whereas the substrate gages show negative (lagging) values for $\phi_\tau$.

As with all experimental results, the results for $\tau_1/\tau_m$ and $\phi_\tau$ in Figs. 7b and 7c indicated by the three hot-element gages involve uncertainties. Evaluation of these uncertainties is quite complex since separate but related measurements were involved in determining $\tau(t)$ indicated by a given gage. For example, a 1% bias error in measuring velocities in a steady boundary-layer velocity profile results in a 2% error in wall shear stress derived from the profile, which in turn is reflected in the hot-element gage calibration constants. Although $\tau_1$ and $\tau_m$ may vary somewhat for repeated experiments and gage calibrations, variations in results are small when the ratio $\tau_1/\tau_m$ is considered. This was also evident in evaluation of the phase angle $\phi_\tau$. The results for $\phi_\tau$ were essentially independent of the values obtained for $\tau_m$ and $\tau_1$. In addition, since the gages operate in a high-turbulence-level environment, the values for $\phi_\tau$ are particularly sensitive to the number of cycles over which ensemble averaging is applied. Errors in $\phi_\tau$ are minimized by taking data for the large number of cycles noted earlier. Based on repeated experiments performed in assessing gage response, the estimated uncertainty from all factors for $\tau_1/\tau_m$ is about ±4%. The estimated uncertainty in measured $\phi_\tau$ values is about ±1 deg. These values also apply to the predictions made by the instantaneous velocity profile method.

As noted, the results obtained using the computer code in Figs. 7b and 7c differ somewhat from results predicted by the instantaneous velocity profile method. The computer code results are based on a relatively simple turbulence model and thus would not be expected to yield exact results. For this reason it is believed that the predictions by the computer code are less reliable. Nonetheless, the computer code results are useful because they provide independent results that confirm the trend predicted by the velocity profile method.

In summary, it is evident from the results in Fig. 7 that when steady-flow calibrations are used to interpret anemometer output signals, the substrate-type gages fail to indicate correctly both the amplitude and phase angle of the wall shear stress variation in the frequency range investigated. The cavity gage exhibits significantly better response characteristics; only the phase angle differs to a significant degree from the predictions. In addition, the relatively poor response characteristics exhibited by the two substrate gages in oscillating flows are consistent with the long response times exhibited by these gages in the steplike flow. Also, as noted for the steplike flow, the response of the glue-on gage was somewhat more rapid than the quartz-substrate gage. The same trend exists for the oscillating flows. The glue-on gage exhibits slightly better response characteristics relative to the quartz-substrate gage, as evidenced by the somewhat larger $\tau_1/\tau_m$ values and more positive values for $\phi_\tau$.

The results in Fig. 7 can be used to obtain approximate corrections for the oscillating-flow response of the gages studied. The corrections presented here are based on the wall shear stress variation predicted by the instantaneous velocity profile method. Figure

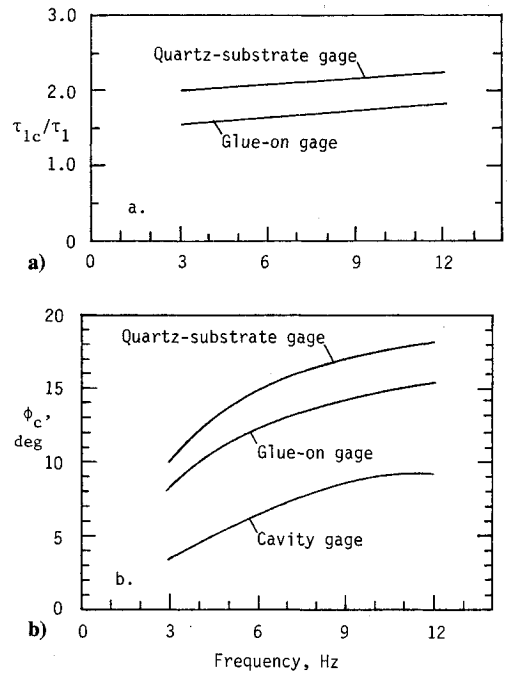


**Fig. 8 Corrections to gage response for oscillating flows.**

8a presents corrections for the wall shear stress amplitude for the substrate gages. The figure shows the ratio $\tau_{1c}/\tau_1$ vs frequency, where $\tau_{1c}$ is the corrected wall shear stress and $\tau_1$ is the amplitude of the ensemble-averaged shear stress variation obtained from processing the gage signal using gage calibration obtained for steady flow. The uncertainty in the amplitude corrections is estimated to be ±5%. In view of the good agreement in Fig. 7b between the amplitudes indicated by the cavity gage and the reference amplitudes, the amplitude correction factor for this gage is essentially unity for the frequency range investigated.

Figure 8b presents the corresponding correction curves to $\phi_\tau$ for both the cavity gage and the substrate gages. These corrections should be added to the phase angle obtained for the ensemble-averaged wall shear stress variation for the particular gage. The uncertainty in the angle correction curves is estimated to be about ±1.5 deg. The trends of the curves, particularly that for the cavity gage, suggest for frequencies approaching zero that the phase angle correction goes to zero. However, the trend of the amplitude correction curves in Fig. 8a is not toward unity as frequency approaches zero. The results for the response of the substrate gages to the steplike flow shown in Figs. 4c and 4d suggest that the period of oscillation would have to be on the order of tens of seconds for the amplitude correction factor to approach unity.

## VIII. Summary and Conclusions

The response characteristics of two types of hot-element gages have been studied for two unsteady turbulent airflows: a steplike flow and an oscillating flow. Data taken in the unsteady flows were reduced using hot-element gage calibrations determined for steady flows. The substrate-type gages exhibited response times on the order of tens of seconds to the steplike flow. The glue-on gage showed slightly better response to the step when compared with the quartz-substrate gage. The response time of the cavity gage in the same flow is on the order of a fraction of a second. The 12% wall shear stress turbulence level for steady flows indicated by the substrate gages is considerably lower than the 28% indicated by the cavity gage, which in turn is lower than the expected 40% turbulence level. For oscillating turbulent flows with frequencies ranging from 3 to 12 Hz, both the substrate-type gages and the cavity gage indicate mean shear stress levels that agree well with the shear stress determined for a steady flow having the same mean velocity profile. However, the substrate gages indicate amplitudes that are about half of the actual amplitudes, whereas the cavity

gage measures amplitude variations that are in good agreement with actual values. Results show that each hot-element gage exhibits some phase lag in oscillating flows; the substrate gages exhibit the largest and the cavity gage exhibits the smallest. The response characteristics of the glue-on gage are slightly better than those of the quartz-substrate gage when the gages are operated in oscillating flows. Changing the overheat ratio for the quartz-substrate gage did not affect the response characteristics of the gage for either the steplike or the oscillating flows. The results obtained for the oscillating flow are consistent with those obtained for the steplike flow. Both sets of results show that the glue-on gage is slightly more responsive to unsteady flows than is the quartz-substrate gage. However, the results clearly show for the range of this study that in unsteady turbulent airflows the cavity gage has good response, whereas the substrate-type gages generally have poor response characteristics. The results suggest that for the substrate-type gages subjected to oscillating airflows the poor response extends to frequencies below the lowest frequency examined in this study.

## Acknowledgment

The author is indebted to Robert Houdeville, ONERA, Toulouse, France, for supplying the cavity gage tested in this study.

## References

[1]Winter, K. G., "An Outline of Techniques Available for the Measurement of Skin Friction in Turbulent Boundary Layers," *Progress in Aerospace Sciences,* Vol. 18, No. 1, 1977, pp. 1–57.

[2]Settles, G., "Recent Skin Friction Techniques for Compressible Flows," AIAA Paper 86-1009, May 1986.

[3]Cole, K. D., and Beck, J. V., "Conjugated Heat Transfer From a Hot-Film for Transient Air Flow," *Journal of Heat Transfer,* Vol. 110, May 1988, pp. 290–296.

[4]Cook, W. J., Giddings, T. A., and Murphy, J. D., "Response of Hot-Element Wall Shear-Stress Gauges in Laminar Oscillating Flows," *AIAA Journal,* Vol. 26, No. 6, 1988, pp. 706–713.

[5]Alfredsson, P. H., Johansson, A. V., Haritonidis, J. H., and Eckelmann, H., "The Fluctuating Wall-Shear Stress and Velocity Field in the Viscous Sublayer," *Physics of Fluids,* Vol. 31, No. 5, 1988, pp. 1026–1033.

[6]Ludwieg, H., "Instrument for Measuring the Wall Shearing Stress of Turbulent Boundary Layers," NACA TM 1284, May 1950.

[7]Liepmann, H. W., and Skinner, G. T., "Shearing Stress Measurements by Use of a Heated Element," NACA TN 3268, Nov. 1954.

[8]Bellhouse, B. J., and Schultz, D. L., "The Measurement of Skin Friction in Supersonic Flow by Means of Heated Thin Film Gauges," Aeronautical Research Council R & M 3490, London, Oct. 1965.

[9]Bellhouse, B. J., and Schultz, D. L., "Determination of Mean and Dynamic Skin Friction, Separation and Transition in Low-Speed Flow with a Thin-Film Heated Element," *Journal of Fluid Mechanics,* Vol. 24, 1966, Pt. 2, pp. 379–400.

[10]Owen, F. K., and Bellhouse, B. J., "Skin-Friction Measurements at Supersonic Speed," *AIAA Journal,* Vol. 8, No. 7, 1970, pp. 1358–1360.

[11]Owen, F. K., and Johnson, D. A., "Separated Skin Friction Measurement—Source of Error, Assessment, and Elimination," AIAA Paper 80-1409, July 1980.

[12]Stack, J. P., Mangalam, S. M., and Berry, S. A., "A Unique Measurement Technique to Study Laminar-Separation Bubble Characteristics on an Airfoil," AIAA Paper 87-1271, June 1987.

[13]McCroskey, W. J., and Durbin, E. J., "Flow Angle and Shear Stress Measurements Using Heated Films and Wires," *Transactions of the ASME, Journal of Basic Engineering,* Vol. 94, March 1972, pp. 46–52.

[14]Houdeville, R., Juillen, J. C., and Cousteix, J., "Skin Friction Measurements with Hot-Element Gages," *Recherche Aerospatiale,* Vol. 1, 1984, pp. 67–79.

[15]Cook, W. J., "Experience With Hot-Wire Measurements in Oscillating Turbulent Boundary Layers," *Proceedings of the Symposium on The Heuristics of Thermal Anemometry,* edited by D. Stock, S. Sherif, and A. Smits, ASME-FED-Vol. 97, American Society of Mechanical Engineers, 1990, pp. 9–16.

[16]Ludwig, H., and Tillman, W., "Investigations of the Wall-Shearing Stress in Turbulent Boundary Layers," NACA TM 1285, May 1950.

[17]Mautner, T. S., and Van Atta, C. W., "Wall Shear Stress Measurements in the Plane of Symmetry of a Turbulent Spot," *Experiments in Fluids,* Vol. 4, No. 3, 1986, pp. 153–162.

[18]Patel, M. H., "On Turbulent Boundary Layers in Oscillating Flow," *Proceedings of the Royal Society of London, Series A—Mathematical and Physical Sciences,* Vol. 353, Feb. 1977, pp. 121–144.

[19]Cousteix, J., Houdeville, R., and Javelle, J., "Response of Turbulent Boundary Layer to a Pulsation from the External Flow With and Without Adverse Pressure Gradient," *Unsteady Turbulent Shear Flows,* edited by R. Michel, J. Cousteix, and R. Houdeville, Springer-Verlag, New York, 1981, pp. 120–144.

[20]Purtell, L. P., Klebanoff, P. S., and Buckley, F. T., "Turbulent Boundary Layer at Low Reynolds Number," *Physics of Fluids,* Vol. 24, No. 5, 1981, pp. 802–811.

[21]White, F. M., *Viscous Fluid Flow,* McGraw-Hill, New York, 1974.

[22]Murphy, J. D., and Prenter, P. M., "A Hybrid Computing Scheme for Unsteady Boundary Layers," *Third Symposium on Turbulent Shear Flows,* Univ. of California, Davis, Davis, CA, 1981.

[23]Cebeci, T., and Smith, A. M. O., "A Finite Difference Solution of the Incompressible Turbulent Boundary Layer Equations by an Eddy Viscosity Concept," *Proceedings, Computations of Turbulent Boundary Layers,* AFOSR-IFP- Stanford Conference, Stanford, CA, Aug. 1968, pp. 346–355.